The Rho GTPase Rac1 is Required for Proliferation and Survival of Progenitors in the Developing Forebrain

Dino P. Leone,[1] Karpagam Srinivasan,[1] Cord Brakebusch,[2] Susan K. McConnell[1]

[1] Department of Biology, Stanford University, Stanford, California 94305

[2] Biomedical Institute, BRIC, University of Copenhagen, Copenhagen, Denmark 2100

Received 8 January 2010; revised 1 April 2010; accepted 11 May 2010

ABSTRACT: **Progenitor cells in the ventricular zone (VZ) and subventricular zone (SVZ) of the developing forebrain give rise to neurons and glial cells, and are characterized by distinct morphologies and proliferative behaviors. The mechanisms that distinguish VZ and SVZ progenitors are not well understood, although the homeodomain transcription factor Cux2 and Cyclin D2, a core component of the cell cycle machinery, are specifically involved in controlling SVZ cell proliferation. Rho GTPases have been implicated in regulating the proliferation, differentiation, and migration of many cell types, and one family member, Cdc42, affects the polarity and proliferation of radial glial cells in the VZ. Here, we show that another family member, Rac1, is required for the normal proliferation and differentiation of SVZ progenitors and for survival of both VZ and SVZ progenitors. A forebrain-specific loss of Rac1 leads to an SVZ-specific reduction in proliferation, a concomitant increase in cell cycle exit, and premature differentiation. In Rac1 mutants, the SVZ and VZ can no longer be delineated, but rather fuse to become a single compact zone of intermingled cells. Cyclin D2 expression, which is normally expressed by both VZ and SVZ progenitors, is reduced in Rac1 mutants, suggesting that the mutant cells differentiate precociously. Rac1-deficient mice can still generate SVZ-derived upper layer neurons, indicating that Rac1 is not required for the acquisition of upper layer neuronal fates, but instead is needed for the normal regulation of proliferation by progenitor cells in the SVZ.** © 2010 Wiley Periodicals, Inc. Develop Neurobiol 70: 659–678, 2010

Keywords: **brain; development; cortex; proliferation; progenitor**

INTRODUCTION

During development, the mammalian cerebral cortex must produce a multitude of neuronal and glial cell types. The traditional view of corticogenesis held that neurons are generated by a pool of progenitors that line the lateral ventricles, called the ventricular zone (VZ), whereas glia are produced in the subventricular zone (SVZ), positioned just above the VZ (Bayer and Altman, 1991). However, SVZ cells and neurons of layers 2–4 express a number of markers in common, including Cux1, Cux2, and the non-coding mRNA Svet1 (Tarabykin et al., 2001; Nieto et al., 2004), suggesting that the SVZ might give rise to upper layer neurons. Indeed, time-lapse imaging and genetic experiments support this view, showing that late-generated neurons are derived from intermediate progenitors in the SVZ (Haubensak et al., 2004; Miyata et al., 2004; Noctor et al., 2004). Evolutionarily, the SVZ appears to be a mammalian solution for the radial expansion and production of layers 2–4 of the

Additional Supporting Information may be found in the online version of this article.

Correspondence to: S.K. McConnell (suemcc@stanford.edu).

Contract grant sponsor: NIMH; contract grant number: MH51864.

Contract grant sponsor: Swiss National Science Foundation.

Published online 18 May 2010 in Wiley InterScience (www.interscience.wiley.com).
DOI 10.1002/dneu.20804

cerebral cortex, developed after mammals segregated from a common ancestor shared with reptiles (which lack layers 2–4; reviewed in Zardoya and Meyer, 2001).

SVZ progenitors are distinct in their morphology, organization, and behavior during the cell cycle compared to precursors in the VZ. The VZ consists of radial glial cells that are organized into a tightly packed pseudostratified epithelium. Each cell extends a long process to the marginal zone that anchors the cell to the pial surface and an apical process that contacts the ventricle (reviewed in Rakic, 2003a,b). As VZ cells progress through the cell cycle, their nuclei undergo interkinetic migration, shuttling between the basal boundary of the VZ during S-phase and the apical surface during M-phase, and producing either equal daughter cells through symmetric divisions or unequal daughter cells through asymmetric divisions (Chenn and McConnell, 1995; Chenn et al., 1998; Miyata et al., 2001; Miyata et al., 2004; Noctor et al., 2004; Noctor et al., 2008). In the SVZ, in contrast, progenitors are loosely packed and exhibit a multipolar morphology. They can undergo mitosis at any position within the SVZ, but these are generally symmetric divisions that produce either two more progenitors or two differentiating upper layer neurons (Noctor et al., 2004).

The mechanisms that distinguish the proliferative behavior of VZ and SVZ progenitors are not well understood, but at least part of the difference is governed by the homeodomain transcription factor Cux2, which is expressed in SVZ but not VZ cells. The genetic disruption of Cux2 in mice specifically alters the proliferation of SVZ progenitors, which show an increased rate of reentry into the cell cycle and produce excessive numbers of upper layer neurons in mutants (Cubelos et al., 2008). Cux2 thus appears to control the proliferation of SVZ progenitors and thereby regulate the number of upper layer neurons that are produced during development. Whether and how Cux2 interacts with factors that regulate cell cycle progression and differentiation remains unknown.

Interestingly, VZ and SVZ cells differ in their expression of core components of the cell cycle machinery. The two primary mid-G1 phase cyclins in the developing cortex are cyclin D1 and D2 (Ross et al., 1996; Wianny et al., 1998; Glickstein et al., 2007). Cyclin D1 is expressed by VZ cells but not by those in the SVZ (Glickstein et al., 2007). Cyclin D2, in contrast, is expressed at E12.5 primarily in abventricular VZ cells, the somata of which are displaced from the ventricular surface, starting at E14.5 is expressed exclusively in the emerging SVZ (Glickstein et al., 2007). Cyclin D2 knockout mice show a 20% reduction in Tbr2-positive SVZ progenitors along with decreased proliferation and increased cell cycle exit by SVZ cells (Glickstein et al., 2009). Thus, while cyclin D2 is not absolutely necessary for the survival or cell cycle progression of SVZ cells, it is required to expand the SVZ by driving proliferation.

To examine potential regulators of the proliferation of SVZ and VZ progenitors, we took a candidate approach and focused on the Rho family GTPase Rac1, since Cdc42, another Rho GTPase, regulates the polarity and mitotic behavior of progenitors in the VZ (Cappello et al., 2006). Rho GTPases regulate proliferation in several systems (reviewed in Etienne-Manneville and Hall, 2002). Rac1 and Cdc42 share many effectors and Cdc42 has been shown to positively control Rac1 activation, suggesting that Rac1 might mediate some of the aspects of Cdc42 function. On the other hand, Rac1 has been shown to regulate proliferation independently of Cdc42; for example, in the skin, it was shown that Rac1 negatively regulates c-Myc via autophosphorylation of p21-activated kinase 2 (PAK2), a downstream effector of Rac1 (Benitah et al., 2005). Deletion of Rac1 in epidermal stem cells leads to a loss of PAK2, and a concomitant depletion of the stem cell pool due to terminal differentiation of progenitors (Benitah et al., 2005). Another study has described Rac1's role in the maintenance of hair follicle integrity, but showed that it is dispensable for maintenance of the epidermis (Chrostek et al., 2006).

Interactions between Rac1, PAK, and c-Myc in non-neuronal cells raise the possibility that Rac1 may regulate cell cycle progression in the nervous system. Rac1 mRNA is ubiquitously expressed in the developing brain (Olenik et al., 1999), as are C-myc and N-myc (Knoepfler et al., 2002). Loss of N-myc leads to severely reduced proliferation and precocious differentiation in the developing cerebral cortex, along with a striking reduction in the myc target gene cyclin D2 in the developing cerebellum and increased levels of the cdk inhibitors p27kip1 and p18ink4c (Knoepfler et al., 2002). Interestingly, Rac1 regulates cyclin D2 expression in B-cells (Glassford et al., 2001), although through an as yet unknown pathway. Animals in which Rac1 was knocked out using conventional gene targeting methods die before E9.5, thereby precluding loss-of-function analysis of Rac1 during forebrain development (Sugihara et al., 1998). However, one study in which a conditional allele of Rac1 was deleted in the developing forebrain suggests that Rac1 regulates the proliferation of cortical progenitors (Chen et al., 2009). However, that study

presents conflicting data showing both decreased numbers of progenitors as assessed by Ki67 staining and increased numbers of mitotic cells using the M-phase marker phosphorylated histone 3. Because these data are difficult to reconcile, and to further examine the role of Rac1 in the proliferation and differentiation of VZ versus SVZ progenitors, we took advantage of a previously published conditional Rac1 allele (Chrostek et al., 2006) and crossed these mice with animals expressing Cre under the control of the Foxg1 locus (Foxg1-Cre; Hébert and McConnell, 2000), thereby ablating Rac1 function in the developing forebrain. In these animals (Foxg1-Cre; $Rac1^{fx/fx}$, referred to as cKO Rac1 mice), Cre-mediated recombination starts as early as E8.5 in the anterior neural ridge, and by E9.5 recombination can be detected throughout the entire telencephalic vesicle (Hébert and McConnell, 2000). We find that cKO Rac1 mice exhibit smaller brains, apoptosis in both VZ and SVZ progenitor populations, and a marked reduction in the proliferation of SVZ cells, but not VZ cells, accompanied by the precocious differentiation of SVZ progenitors. Furthermore, loss of Rac1 leads to disruptions in the basal lamina that are associated with cobblestone-like migration defects, in which displaced neurons invade the pericerebral space.

METHODS

Animals

Rac1 cKO mice were obtained by breeding animals hemizygous for Foxg1-Cre (Hébert and McConnell, 2000) and heterozygous for floxed Rac1 ($Rac1^{fx}$) with homozygous $Rac1^{fx/fx}$ mice, thereby producing control (Foxg1-Cre^{+}; $Rac1^{fx/wt}$) and mutant animals (Foxg1-Cre^{+};$Rac1^{fx/fx}$). Animals were genotyped by PCR as previously described (Hébert and McConnell, 2000; Chrostek et al., 2006).

For the tamoxifen-inducible Nestin-CreERT2 experiments, mice hemizygous for Z/EG (Novak et al., 2000) and homozygous for Rac1 ($Rac1^{fx/fx}$; Z/EG^{+}) were mated with animals hemizygous for the Nestin-CreERT2 (Imayoshi et al., 2006), producing F1 offspring that carried the Nestin-CreERT2 and Z/EG on a $Rac1^{fx}$ heterozygous background (NesCre^{+};$Rac1^{fx/wt}$;Z/EG^{+}). These F1 offspring were then mated with homozygous $Rac1^{fx/fx}$ females producing mutant offspring (Nestin-$CreERT2^{+}$;$Rac1^{fx/fx}$;Z/EG^{+}) and controls (Nestin-$CreERT2^{+}$;$Rac1^{fx/wt}$;Z/EG^{+}). Tamoxifen (Sigma) was dissolved in DMSO at 10 mg/mL and pregnant dams were injected with a single intraperitoneal dose of 1 mg at E11.5. Animals were genotyped by PCR for Cre [primers 5′-aggctaagtgccttctctacac-3′ (Cre-antisense) and 5′-accaggttcgttcacgcatgg-3′ (Cre-sense)] and Z/EG [primers 5′-gtaaacggccacaagttcag-3′ (GFP-forward) and 5′-tcgttggggtctttgctcag-3′ (GFP-reverse)].

BrdU was injected into pregnant females at 50 mg/kg body weight. For timed matings the morning of vaginal plug observation was defined as E0.5.

Histology, Immunohistochemistry, and *In Situ* Hybridization

Brains and embryos were fixed in 4% paraformaldehyde/PBS overnight, cryoprotected in 30% sucrose/PBS for 24–48 h before embedding in Tissue-Tek OCT, and cryosectioned at 15–20 μm on a Leica CM1900 cryostat. Sections were incubated overnight at 4°C with primary antibodies, and 1–2 h at room temperature with secondary antibodies. Primary antibodies used included: mouse-anti Satb2 (1:200; abcam), rabbit-anti Ctip2 (1:50; Novus Biological), mouse-anti Nestin (1:100; Pharmingen), mouse-anti Reelin (1:100; Millipore), Laminin (1:50; Sigma), rabbit-anti Tbr2 (1:250; Chemicon and abcam), rat-anti BrdU (1:500; Accurate Chemical), mouse-anti Ki67 (1:500, Pharmingen), mouse-anti TuJ1 (1:500; Covance), rabbit anti-GFP (1:2000; Molecular Probes) rabbit-anti Cadherins (1:500; Sigma), mouse-anti beta-catenin (1:500; Transduction Laboratories), mouse-anti ZO1 (1:100; Developmental hybridoma bank), rabbit-anti Lin7 [1:1000; (Srinivasan et al., 2008)], rabbit-anti P-PAK (1:100; Cell Signaling), anti-DIG peroxidase (1:500, Roche). Secondary antibodies used were Alexa555-conjugated goat anti-rabbit, Alexa488-conjugated goat anti-mouse, Alexa680-conjugated goat anti-rabbit, and Alexa594-conjugated goat anti-rabbit. All secondary antibodies were used at 1:500.

Immunohistochemical staining against Tbr2 using the anti-Tbr2 antibody from Chemicon required antigen retrieval by boiling the sections for 30 min in 10 m*M* sodium citrate. For BrdU staining, sections were treated with 2 *N* HCl at 37°C for 25 min, and washed three times in PBS before incubation with the primary antibody. All sections were counterstained with DAPI. Images were collected on a Zeiss META confocal microscope and processed using ImageJ and Adobe Photoshop.

TUNEL staining was carried out according to manufacturer's protocol (Roche).

For cresyl violet staining tissue was fixed in Carnoy's fixative (60% ethanol, 30% chloroform, and 10% acetic acid) overnight, dehydrated in ascending grades of ethanol, cleared in xylene, and embedded in paraffin. Sections cut at 10 μm and mounted on gelatine-coated slides. Paraffin sections were dewaxed, rehydrated, and then stained.

In situ hybridization using ^{35}S-labeled probes was performed as previously described (Frantz et al., 1994; Hébert et al., 2003). For fluorescent digoxygenin (DIG) *in situ* hybridization, probes were labeled according to the manufacturer's directions (DIG RNA labeling Kit; Roche). Sections were air dried for 10 min before postfixing them in 4% PFA/PBS for 10 min, washed and acetylated for 10 min using 500 μL Triethanolamine in 5 m*M* HCl in DEPC-treated water. After three wash steps in PBS, slides were pre-hybridized for 2–4 h at room temperature (RT) in hybridization buffer (50% formamide, 5× SSC, 5× Den-

hardt's, 0.5 mg/mL herring sperm DNA, and 25 μg/mL yeast tRNA). After the DIG-labeled riboprobes were denatured for 5 min at 80°C and chilled on ice, the sections were incubated with the DIG-labeled probes in hybridization solution overnight in a moist chamber at 70°C. After hybridization, sections were washed (2× SSC at RT for 5 min, then 0.2× SSC at 70°C for 1 h, and finally 10 min at RT in 0.1 *M* Tris-HCl pH 7.5, 0.15 *M* NaCl). After the washes, sections were incubated in blocking buffer according to manufacturer's directions (DIG RNA labeling kit; Roche) and incubated overnight at 4°C with both a primary antibody against a particular antigen and the primary anti-DIG peroxidase antibody in blocking buffer. The following day, sections were washed three times in 0.1% Triton/PBS, followed by tyramide amplification according to manufacturer's directions (TSA Plus Cyanine 3 System; Perkin Elmer). After the tyramide detection step, sections were incubated with a secondary antibody according to standard immunohistochemical protocols for detection of the corresponding antigen that was probed for in the primary antibody incubation step.

Riboprobes were generated by RT-PCR from E15.5 brain cDNA. The sequences of the primers for the riboprobes used were:

Cyclin D1: 5′-atcatctagccatgcacgag-3′ and 5′-cagcttgctagggaacttgg-3′

Cyclin D2: 5′-ctggatcccatcttgttgct-3′ and 5′-tggcttcgtaaaaccagagc-3′

Cyclin E1: 5′-gtctgcaagatgccttggat-3′ and 5′-ccacacttgctcacaaccac-3′

p18: 5′-agcagccaaatccttcaaaa-3′ and 5′-gcaaaagatgcatcaggaca-3′

p21: 5′-aagtgggattccctggtctt-3′ and 5′-gctttgacacccacggtatt-3′

p27: 5′-ctcaccctctttgacccaga-3′ and 5′-cagcttcgggaagaagattg-3′

p57: 5′-acgcaactgctgggttattg-3′ and 5′-ccatttcgactgtctggtca-3′

Svet1: 5′-gtcctcagacaaccggagtg-3′ and 5′-catacctgccatgcaaacac-3′

Myc: 5′-tgtccattcaagcagacgag-3′ and 5′-gctgaagcttacagtcccaaa-3′

N-Myc: 5′-gctcttgcggccagtattag-3′ and 5′-acccagttctatgcaccaaa-3′

Cux1: 5′-gggcaacagctggaaataaa-3′ and 5′-ttcttggcattcagttgctg-3′

Cux2: 5′-aggacaccctcgtgacagac-3′ and 5′-tggggaagaagacatccttg-3′.

RESULTS

Morphological Defects in Rac1-Deficient Forebrains

Although Rac1 mRNA is expressed at early stages of corticogenesis (E13.5) (Olenik et al., 1999; and data not shown), we did not observe any obvious morphological defects at this age in cKO Rac1 mutants, as assessed by cresyl violet staining [Supporting Information Fig. 1(A,B)] or immunohistochemistry against the neuronal marker TuJ1 [Supporting Information Fig. 1(C,D)], suggesting that the early generation of neurons is unaffected by the absence of Rac1. At E17.5, however, mutant brains appeared significantly smaller than controls in whole-mount preparations [Fig. 1(A,B)]. Quantification of the size differences revealed that the mutant cortices were significantly smaller along both the anterior–posterior and medial–lateral axes [Fig. 1(C)]. On average, the length of control brains along the anterior–posterior axis was 4.26 ± 0.02 mm, whereas mutants averaged 3.87 ± 0.05 mm ($n = 5$ mutants and $n = 5$ controls; $p < 3 \times 10^{-5}$; one-tailed, unpaired t test). The difference between mutants and controls was even more pronounced when the cortices were measured in the medial–lateral dimension; controls averaged 2.27 ± 0.03 mm, whereas mutants averaged 1.73 ± 0.08 mm [$p < 0.0002$; one-tailed, unpaired t test; Fig. 1(F)]. The olfactory bulbs in Rac1 cKO brains are almost completely absent [Fig. 1(B)], indicative of either a migration defect in the rostral migratory stream, similar to a previous report describing the role of the transcription factor serum response factor (SRF; Alberti et al., 2005), or alternatively, the reduced size of the olfactory bulb could be due to a defect in proliferation in the initial bulb evagination, as described previously (Hébert et al., 2003).

Coronal sections through the forebrain revealed an overall reduction in the thickness of the cerebral wall [Fig. 1(D,E)] accompanied by defects in its radial organization. The VZ, SVZ, and intermediate zone (IZ) appeared to be reduced in thickness [Fig. 1(E)], and VZ progenitors were no longer as tightly packed or radially oriented as in controls, instead resembling the more loosely packed SVZ, which made a demarcation of VZ and SVZ impossible in Rac1 cKOs. Previous studies have shown that a forebrain-specific ablation of another Rho GTPase family member, Cdc42, leads to a disorganization of the radial glial cells within the VZ, associated with a loss of adherens junctions and the apical Par protein complex (Cappello et al., 2006 and unpublished observations, DPL and SKM). We therefore tested whether changes in adherens junctions or the localization of polarized proteins might be disrupted in Rac1 mutants. We first assessed the localization of cadherins, which form an integral component of adherens junctions, and the signaling protein beta-catenin, as changes in their localization could be indicative of adherens junction breakdown (Chenn and Walsh, 2003). However, we observed no obvious differences between the expres-

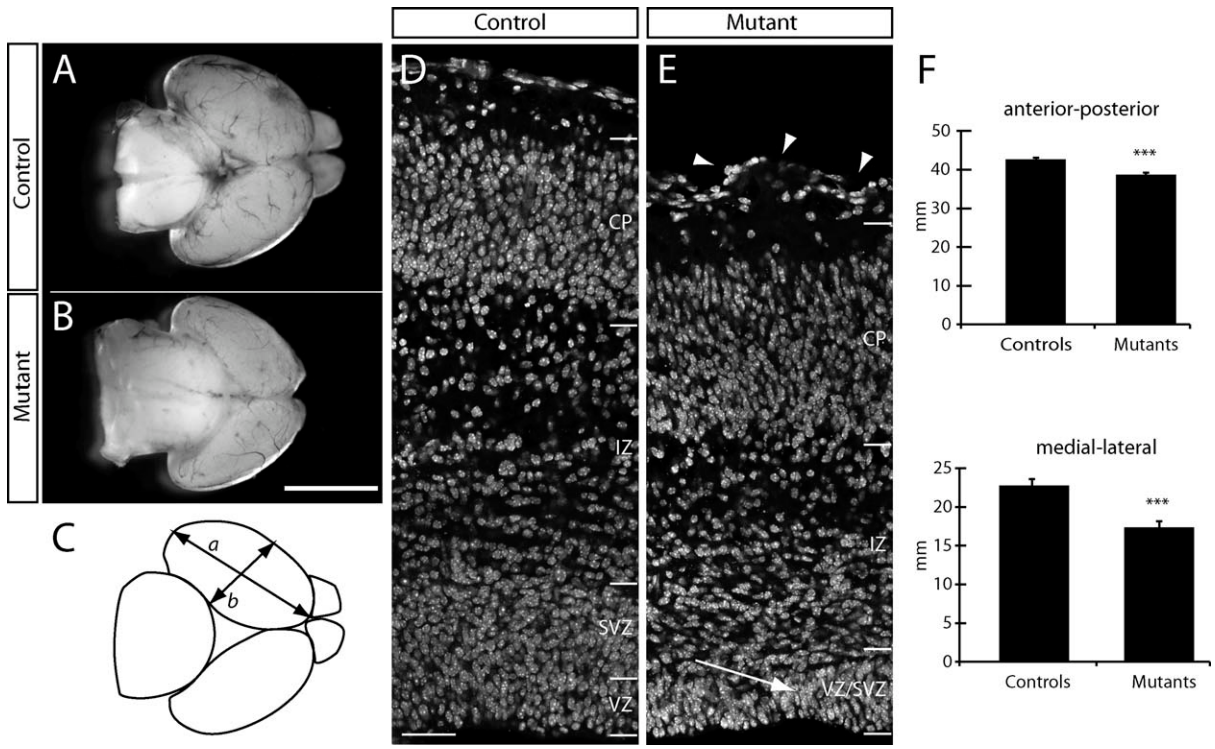

Figure 1 Structural defects in Rac1-deficient brains. Foxg1-Cre-mediated loss of Rac1 leads to structural defects in the forebrain during late neurogenic stages. A and B: Whole mount E17.5 brain preparation shows the smaller size of Rac1-deficient brain (B) compared to a control brain (A). Mutant brains display severely reduced olfactory bulbs. C: Schematic of quantification to assess changes in brain sizes. a: anterior–posterior, b: medial–lateral measurements. D and E: Coronal cross sections through the cerebral cortex of a control animal (D) and a mutant brain (E), counterstained with DAPI to visualize cell nuclei. Disorganization in the VZ and SVZ (arrow) and undulations in the pial surface (arrowheads) are hallmarks of the Rac1-deficient brains. F: Quantification of size differences between controls and mutants. Mutants display a statistically significant reduction in length of the cerebral hemispheres (anterior–posterior), as well as a significant reduction in the medial–lateral measurements compared to controls. *** $p < 0.0005$ Student's t test. Error bars show Mean ± SE. Genotypes: controls are Foxg1-Cre^{+}; Rac1$^{fx/wt}$, mutants are Foxg1-Cre^{+}; Rac1$^{fx/fx}$. Scale bar: 50 μm in D for D and E.

sion patterns of these two proteins [Supporting Information Fig. 2(A–F)], nor did cKO Rac1 mice display alterations in the localization of the apical proteins ZO1 or MALS3 (LIN-7; Srinivasan et al., 2008) [Supporting Information Fig. 2(G–I) vs. (J–L)]. Taken together, these data suggest that, in contrast to Cdc42 mutants, loss of Rac1 does not affect the polarity of VZ progenitors.

We next investigated whether cKO Rac1 cortices show changes in the phosphorylation state of p21-activated kinase (P-PAK), which is a direct downstream effector of both Rac1 and Cdc42 (Manser et al., 1994). In the developing cortex, P-PAK is normally localized to cells lining the ventricular surface. Conditional mutation of Cdc42 leads to a loss of P-PAK (data not shown); however, loss of Rac1 failed to alter P-PAK expression or localization [Supporting Information Fig. 2(M–P)]. Collectively, these data suggest that Cdc42 and Rac1 perform non-overlapping and non-redundant functions in the neocortex.

Migration Defects in Rac1 Mutants

Rho GTPases have been implicated in regulating the migration of many cell types, including fibroblasts, neutrophils, and astrocytes, by regulating actin polymerization and integrin adhesion complex assembly at the leading edge of migrating cells (reviewed in Etienne-Manneville and Hall, 2002). To explore the role of Rac1 in the migration of cortical neurons, we examined the brains of Rac1 mutants for changes in neuronal positioning that might result from defects in migration. The laminar organization of the cerebral wall was intact in E13.5 embryos. At E17.5, neurons

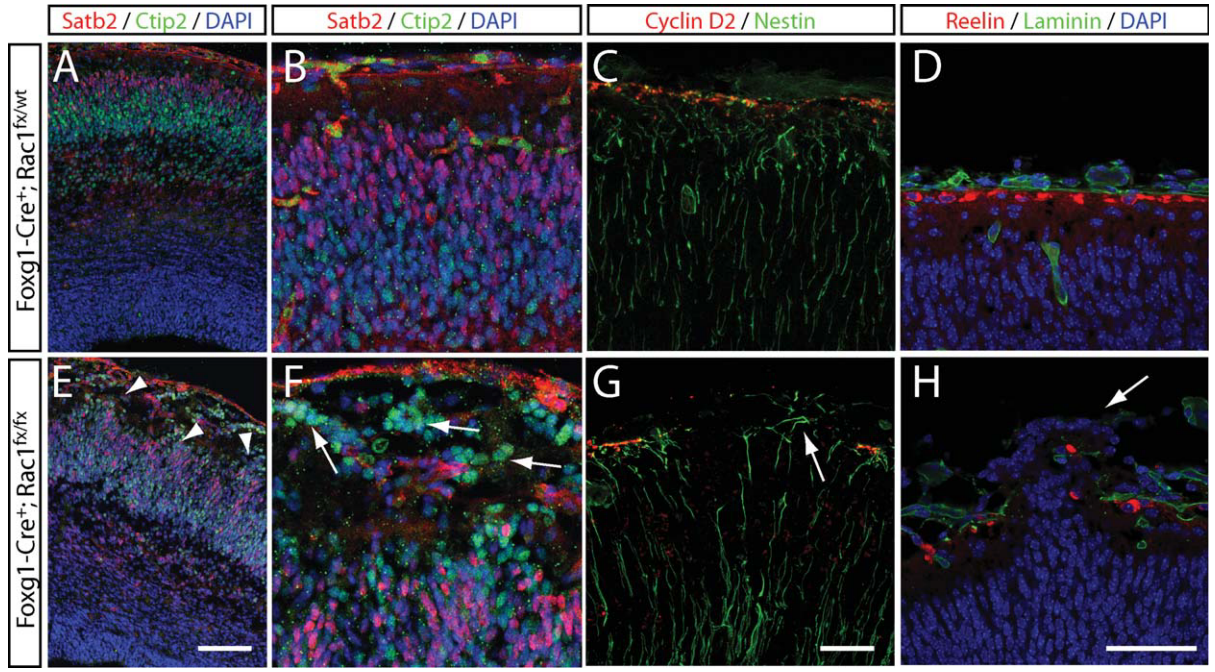

Figure 2 Basement membrane disruptions and migration defects in the developing cortex of Rac1-deficient embryos. A, B, E, and F: The distribution of cells expressing the callosal projection neuron marker Satb2 (red in A, B, E, and F) and the subcortical projection neuron marker Ctip2 (green in A, B, E, and F) show that overall layering is intact in Rac1 mutants (E) compared to controls (A), but undulations (arrowheads in E) and pericerebral invasion of Satb2- and Ctip2-positive neurons in mutants (arrows in F) are visible. Disorganization of radial glia fibers in Rac1-deficient brains is revealed by intermediate filament nestin (green in C and G) and fluorescent *in situ* hybridization against cyclin D2 (labeling pial endfeet; red in C and G). In Rac1 mutants, nestin-positive radial glia (RG) fibers become disorganized (arrow in G), compared to controls (C). Disorganized RG fibers are accompanied by breaks in the Cajal-Retzius layer, as visualized by Reelin (red in D and H) and dispersed localization of laminin (green in D and H) in Rac1-deficient forebrains, leading to ectopic localization of neurons in the pericerebral space (arrow in H). Sections were counterstained with DAPI (blue) to visualize cell nuclei. Genotypes: controls are Foxg1-Cre^{+}; Rac1$^{fx/wt}$, mutants are Foxg1-Cre^{+}; Rac1$^{fx/fx}$. All sections are coronal sections of E17 embryos. Scale bars: 100 μm in E for A and E; 50 μm in G for B, C, F, and G; 50 μm in H for D and H.

expressing Ctip2, a marker for layer 5 and 6 neurons (Arlotta et al., 2005; Chen et al., 2005; Alcamo et al., 2008; Leone et al., 2008), are normally found in lower regions of the cortical plate [Fig. 2(A,B)]. In Rac1-deficient brains, however, many Ctip2-positive cells were found near the pial surface [Fig. 2(E,F); arrowheads and arrows] in addition to those occupying normal deep-layer positions. Neurons expressing Satb2 (a marker for callosally projecting neurons: Britanova et al., 2005; Alcamo et al., 2008; Britanova et al., 2008; Leone et al., 2008) are normally concentrated in the upper layers, and at E17.5 are found in a band at the top of the cortical plate [Fig. 2(A,B)]. In cKO Rac1 mutants, however, Satb2-positive cells were detected throughout the cortical plate [Fig. 2(E)]. These examples of cell body mispositioning are consistent with the possibility that neuronal migration is disrupted by the loss of Rac1.

Mutant brains also displayed undulations in the organization of the cortical plate, with neurons forming small clusters within the marginal zone (MZ) [Fig. 2(E), arrowheads]. Such breaks in the marginal zone and invasion of pericerebral space are reminiscent of many cobblestone lissencephalies (reviewed in Olson and Walsh, 2002). Similar migration disorders have been associated with defects in the basal lamina (Halfter et al., 2002), just below the pial surface, or in the anchoring of radial glia processes to the basal lamina (Voss et al., 2008). We therefore assessed the organization of radial glia in cKO Rac1 brains by examining expression of the intermediate filament nestin. In control cortices, nestin immunoreactivity was present within radial glia fibers, which coursed roughly in parallel out to the pial surface, and at their pial endfeet [Fig. 2(C)]. In Rac1 mutants, radial glial fibers were disorganized, entangled, and often

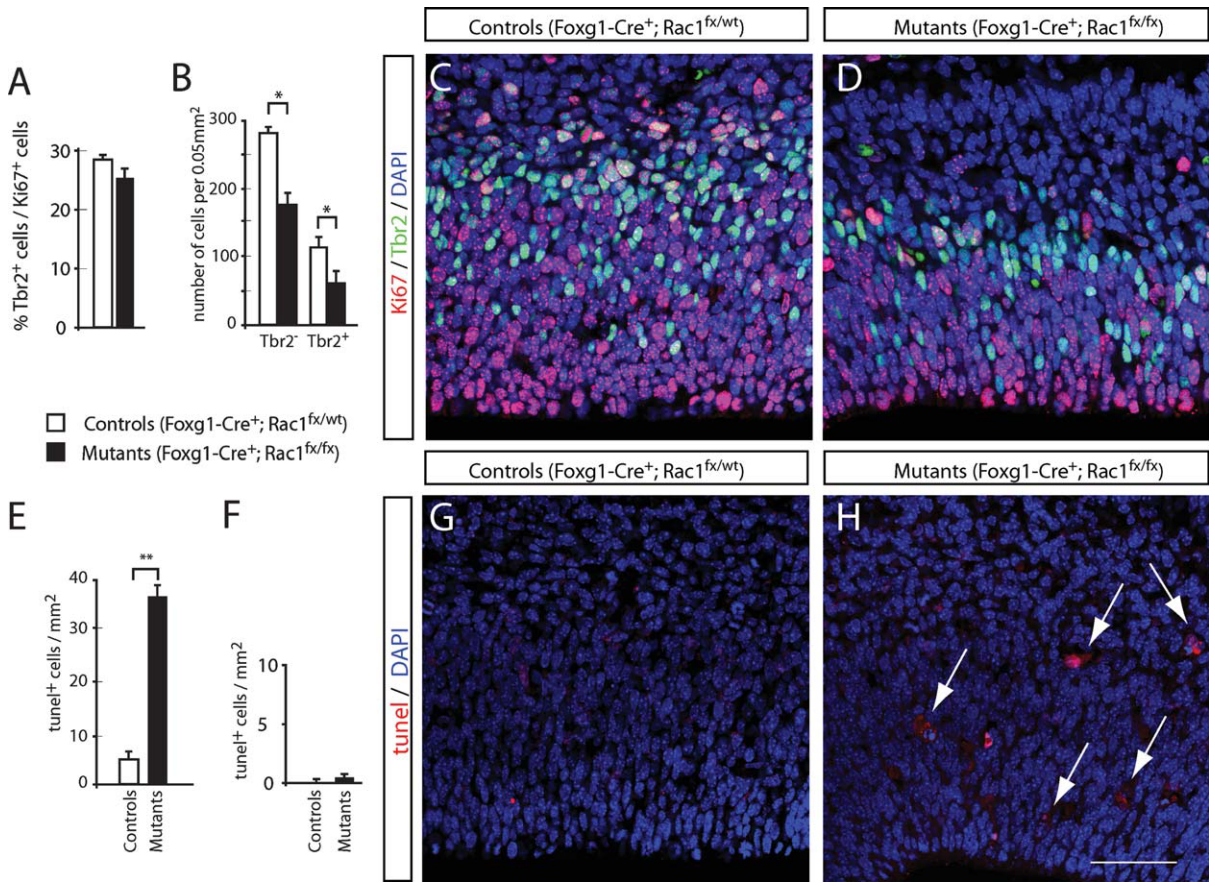

Figure 3 Compaction of SVZ and VZ into a single zone and increased apoptosis in Rac1-deficient brains. A–D: Ki67 and Tbr2 immunohistochemistry on coronal sections of E14.5 controls and mutants reveals changes in the distribution of Tbr2-positive intermediate progenitors. A: No statistically significant difference was found in the percentage of Tbr2-positive cells over the total number of Ki67-expressing cells ($p = 0.28$; Student's t test). B: Rac1 mutants showed a significant reduction in the absolute number of progenitor cells: both $Tbr2^-$ and $Tbr2^+$ cell numbers showed a statistically significant reduction compared to controls [$*p = 0.0015$ ($Tbr2^-$), $*p = 0.022$ ($Tbr2^+$); Student's t test]. C and D: Representative images of coronal sections of E14.5 control (C) and mutant (D) stained against Tbr2 (green) to label intermediate (SVZ) progenitors and Ki67 (red), labeling all proliferating cells. E–H: TUNEL stainings and quantification reveal significant increase in the number of apoptotic cells in Rac1 mutants. E: At E14.5, mutant brains show a statistically significant increase in TUNEL-positive cells compared to controls ($**p < 0.001$; Student's t test). F: At E17.5, no difference in the number of TUNEL-positive cells was detected ($p = 0.02$; Student's t test). G and H: Representative images of coronal sections of E14.5 control (G) and mutant (H) stained for TUNEL (red; arrows). Sections were counterstained with DAPI (blue) to visualize nuclei. Bars show Means ± SE. Scale bar: 50 μm in H for C, D, G, and H.

extended past the marginal zone and into the pericerebral space [Fig. 2(G), arrow]. Normal radial glial cells interact with the basement membrane through their pial endfeet to anchor and maintain their radial morphology. This interaction depends on beta1-integrin (Graus-Porta et al., 2001) and laminin (Beggs et al., 2003). Staining for laminin and the MZ marker reelin revealed coincident breaks in expression within the MZ of Rac1 mutant mice [Fig. 2(D,H)]. These findings suggest that local disorganization within the basement membrane and the resulting loss of radial glia cell attachment are the likely cause of migration defects found in Rac1 mutants. We do not know what role Rac1 plays in the deposition of the basement membrane and/or the stabilization of the pial endfeet of radial glial cells. However, our findings that a significant number of mutant neurons migrate past the pial endfeet into the pericerebral space [Figs. 2(F,H) and 5(F)] suggests a severe defect in the interaction between migrating neurons and the basement membrane.

Changes in Proliferation, Differentiation, and Survival in Rac1 Mutant Brains

One of the most striking changes in the brains of E17.5 Rac1 mutants was the shrinkage and apparent collapse of the VZ and SVZ into a single proliferative zone. Although we did not detect any morphological defects in E13.5 Rac1 deficient brains (Supporting Information Fig. 1) as assessed by cresyl violet staining, Rac1 mutants displayed abnormalities in VZ/SVZ organization in E14.5 sections immunostained for the proliferation marker Ki67 and Tbr2, which marks intermediate progenitors (Englund et al., 2005). In control brains, the majority of Tbr2-positive cells were multipolar cells located in the SVZ, adjacent to the tightly packed VZ. Some Tbr2-positive cells were found in the VZ; presumably these represent newly formed intermediate progenitors destined to migrate into the SVZ [Fig. 3(C)]. In Rac1 mutants, the VZ and SVZ appeared fused into a single zone, disrupting the radially organized pseudostratified columnar epithelium of the VZ [Fig. 3(D)]. The size of the VZ and the number of Tbr2-positive cells appeared reduced. To quantify these findings, we counted the total numbers of $Ki67^{+}$;$Tbr2^{-}$ and $Ki67^{+}$;$Tbr2^{+}$ cells. The fraction of Tbr2-positive cells within the Ki67-positive population was unchanged [Fig. 3(A)], suggesting that the initial generation of intermediate progenitors could occur in the absence of Rac1. However, we found a significant reduction in the absolute numbers of both cell populations in Rac1 mutants [Fig. 3(B); $p = 0.0015$ ($Ki67^{+}$;$Tbr2^{-}$), $p = 0.022$ ($Ki67^{+}$;$Tbr2^{+}$); $n = 3$ controls and 3 mutants], suggesting that Rac1 is required for either proliferation or survival in both cell types.

Rac1 inhibits apoptosis in lymphoma cells (Zhang et al., 2003; Zhang et al., 2004), which raises the possibility that loss of Rac1 could lead to increased apoptosis in cortical progenitors. To address this, we performed TUNEL staining on sections from E14.5 and E17.5 to assess cell death. TUNEL-positive cells were confirmed by double-labeling with DAPI to visualize fragmented nuclei. We found a significant increase in the number of TUNEL-positive cells in Rac1 mutants at E14.5 [Fig. 3(E,H); $p < 0.001$; $n = 5$ controls and 6 mutants], but no difference between mutants and controls at E17.5, suggesting a survival requirement for Rac1 during early corticogenesis.

The disorganization of the VZ and SVZ in E14.5 Rac1 mutants became more pronounced at E15.5, when the fused VZ/SVZ zone formed a single compact, disorganized layer [Fig. 4(G,I)], in contrast to the columnar VZ epithelium and more loosely packed SVZ in controls [Fig. 4(F,H)]. These observations suggest that the boundary between these two zones is lost in Rac1 mutants.

Figure 4 Reduction in proliferative cells in the SVZ and increased fraction of differentiation in the SVZ of Rac1-deficient brains. A: Twenty-four hours after a pulse of BrdU at E15.5, fewer $BrdU^{+}$ cells are seen in the SVZ of Rac1 mutants (SVZ; black bars in A), compared to controls (SVZ; white bars in A) and a concomitant increase in the fraction of $BrdU^{+}$ cells in the intermediate zone (IZ), compared to controls. No significant difference in the percentage of BrdU-labeled cells between mutants and controls were detectable in the VZ, cortical plate (CP), or marginal zone (MZ). B: The labeling index (percent $BrdU^{+}$ cells) after a 2-h BrdU pulse at E15.5 was analyzed separately for the VZ and SVZ using Tbr2 as an SVZ cell marker, revealing a statistically significant reduction in the fraction of proliferating $Tbr2^{+}$ cells in Rac1-deficient brains (black bar, SVZ in B) compared to controls (white bar, SVZ in B). No difference between mutants and controls in BrdU labeling was found for the $Tbr2^{-}$ fraction. C: For Quit fraction analysis (percent cells leaving the cell cycle after a 24-h BrdU pulse), sections were triple-stained against BrdU, Ki67, and Tbr2. At E16.5, a significant increase in the mutant fraction of cells exiting the cell cycle (black bar, $Tbr2^{+}$ in C) was found compared to control $Tbr2^{+}$ cells (white bar, $Tbr2^{+}$ in C). No significant difference between mutant and control quit fractions of $Tbr2^{-}$ progenitors ($Tbr2^{-}$ in C) was found. D: Labeling index at E13.5 reveals no statistically significant difference between controls (white) and mutants (black) at early stage during corticogenesis. E: Quit fraction analysis at E13.5 shows no statistically significant difference in the fraction of cells leaving the cell cycle between mutants (black bar) and controls (white bar). F–I: Representative images of labeling index experiments (at E15.5; used for graphs in B) of a control (F) and a Rac1 mutant brain (G). H and I: High-power magnification views of the ventricular/subventricular zones of E15.5 controls (H) and mutants (I) shows the two zones fused in the mutant with the Tbr2-positive cells shifted towards the apical (ventricular) surface. Sections in F, G, H, and I were triple-stained against BrdU (green; 2-h pulse), Tbr2 (red), and DAPI (blue). Genotypes: all controls are Foxg1-Cre^{+}; $Rac1^{fx/wt}$, mutants are Foxg1-Cre^{+}; $Rac1^{fx/fx}$. *$p < 0.05$, student's t test. Error bars show Mean ± SE. Scale bar: 100 μm in G for F and G, 50 μm in I for H and I.

To explore the proliferation and differentiation of cells that normally occupy these two regions, we injected embryos with BrdU at E15.5 and analyzed the distribution of BrdU-labeled cells 24 h later. Under these conditions, the majority of BrdU-positive cells in controls were located in the SVZ [Fig. 4(A), white bars], with smaller fractions in the VZ and IZ. This was expected because the SVZ acts as a transit amplifying zone in which the progeny of VZ cells pause and undergo additional rounds of cell division to generate the upper layers of cortical neurons (Haubensak et al., 2004; Miyata et al., 2004; Noctor et al., 2004; Englund et al., 2005). Surprisingly, analysis of Rac1 mutant mice revealed a significant deficit in the percentage of BrdU-positive cells in the SVZ/upper VZ [Fig. 4(A), SVZ; $p = 0.013$; $n = 5$ controls and 4 mutants] and a concomitant increase in the fraction of labeled cells in the IZ [Fig. 4(A), IZ; $p = 0.006$] compared to controls. No statistically significant differences were found for the VZ, CP, or MZ. These results raise the possibility that Rac1 mutant cells, unlike their wild-type counterparts, do not pause in the SVZ and undertake additional rounds of cell division, but instead continue their radial migration into the IZ and differentiate precociously.

To determine if the reduced fraction of cells found in the SVZ in Rac1 mutants is the result of decreased proliferation, we first measured the fraction of cells in S-phase (labeling index) within the VZ and SVZ (Srinivasan et al., 2008). Pregnant mice were injected

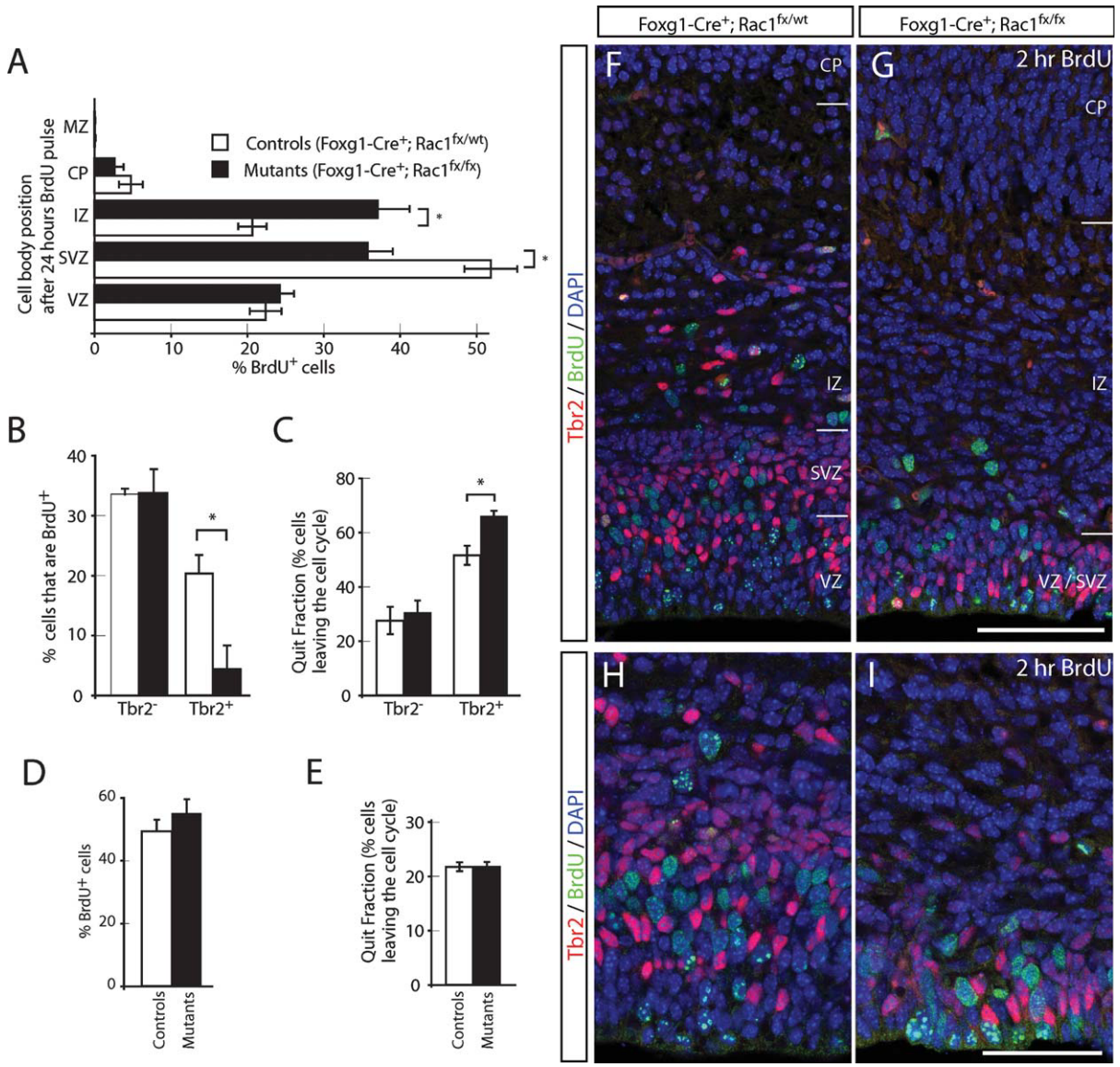

Figure 4

with BrdU at E15.5, and embryos were harvested 2 h later and processed for immunohistochemistry. To distinguish between radial glia and intermediate progenitor (SVZ) divisions, sections were double-stained for Tbr2 (Englund et al., 2005). We counted the fraction of BrdU-positive cells for both the Tbr2-negative and Tbr2-positive populations within the VZ and SVZ [Fig. 4(B); $Tbr2^-$ and $Tbr2^+$]. The fraction of Tbr2-negative cells that incorporated BrdU was nearly identical in mutants and controls [Fig. 4(B): controls, 33.45% ± 0.90%, $n = 3$ animals; mutants 33.70% ± 6.23%, $n = 3$ animals]. For Tbr2-positive intermediate progenitors, however, 20.30% ± 6.70% of cells incorporated BrdU in control mice, whereas only 4.33% ± 4.03% were BrdU-positive in Rac1 mutants ($p = 0.005$; one-tailed Student's t test). These data indicate that the loss of Rac1 specifically affects the proliferation of Tbr2-positive progenitors, but not that of radial glial progenitors in the VZ. This suggests that the Rac1-deficient cortex shows a specific reduction in cell proliferation within the SVZ, where intermediate progenitors normally divide to give rise to upper layer neurons (Noctor et al., 2004).

It is possible that both wild type and mutant VZ progenitors are generated in similar numbers, but that Rac1 mutant SVZ cells differentiate precociously compared to their wild-type counterparts. To assess the percentage of cells that quit the cell cycle and entered terminal differentiation, we measured the quit fractions (QF) for the VZ and SVZ independently. Briefly, 24 h after a BrdU pulse, brains were stained for BrdU (to mark cells that divided within the last cell cycle), Ki67 (which labels all proliferating cells), and Tbr2 (to distinguish between VZ and SVZ progenitors). We define the quit fraction as the fraction of BrdU-positive cells that lack Ki67, which represents progenitor cells that exited the cell cycle and initiated terminal differentiation. An increase in this fraction in Rac1 mutants would suggest that loss of Rac1 results in precocious differentiation at the expense of proliferation. Although we did not detect a significant difference in the quit fraction for VZ cells in mutants versus controls [30.67% ± 8.55% vs. 27.52% ± 10.01%; $n = 4$ controls and 3 mutants; Fig. 4(C)], Rac1-deficient mice showed a significant increase in the quit fraction of $Tbr2^+$ cells compared to their wild-type counterparts [Fig. 4(C), SVZ; 66.22% ± 2.93% vs. 51.56% ± 6.95%; $p = 0.017$; $n = 4$ controls and 3 mutants]. These observations suggest that $Tbr2^+$ cells exit the cell cycle precociously and initiate differentiation, an interpretation consistent with the increased fraction of BrdU-positive cells that occupy the IZ at this time in Rac1 mutant mice [Fig. 4(A)].

In light of the impact that loss of Rac1 has on SVZ progenitors during mid-corticogenesis, we asked whether Rac1 played a similar or distinct role in radial glia at an earlier stage during corticogenesis. We therefore analyzed the neuroepithelium of mice at E13.5 2 h after BrdU incorporation and calculated the labeling index, as described above for older animals. At E13.5, however, there were no statistically significant differences in the percentages of BrdU-positive cells between mutants and controls [Fig. 4(D); $n = 3$ mutants and controls; 55.1% ± 4.41% vs. 49.4% ± 3.56%]. This suggests that the proliferative behavior of progenitors at E13.5 is not affected by loss of Rac1. To investigate whether the early Rac1 progenitors undergo precocious differentiation, we measured the quit fraction as described above, but we detected no significant difference between mutants and controls at this early stage of corticogenesis [Fig. 4(E); 22.8% ± 0.1% vs. 22.0% ± 0.1%; $p = 0.8$; $n = 3$ mutants and 5 controls]. These findings provide strong evidence that the proliferative behavior of VZ cells is not altered in Rac1 mutants. In contrast, Rac1-deficient $Tbr2^+$ progenitors exit the cell cycle and differentiate precociously, leading to a depletion of the $Tbr2^+$ (SVZ) progenitor pool.

Altered Expression of Cyclin D2 in Rac1-Deficient Brains

To assess the mechanisms by which Rac1 affects the mitotic behavior of intermediate progenitors in the SVZ, we asked whether loss of Rac1 results in changes in the expression of cell cycle regulators such as D-type cyclins. Because Cyclins D1 and D2 are the main D-type cyclins expressed during corticogenesis (Glickstein et al., 2007), we performed *in situ* hybridization against Cyclin D1 and D2 on E17 control and mutant brains. In wild-type animals, Cyclin D1 is weakly expressed by cells in the VZ [Fig. 5(C)], whereas cyclin D2 is expressed in both the SVZ and VZ [Fig. 5(A,E)], as well as in the marginal zone, where it labels the pial endfeet of radial glial cells [Fig. 5(E); Glickstein et al., 2007]. Rac1-deficient brains appeared to show reduced cyclin D1 expression [Fig. 5(D)]. Cyclin D2, on the other hand, showed marked changes in expression in the mutants [Fig. 5(B,F)], with a reduction in the SVZ, along a striking acquisition of ectopic expression in the IZ [Fig. 5(B,F), arrows]. As in controls, Cyclin D2 was detected in the marginal zone of mutants, but the expression pattern showed breaks [Fig. 5(B,F); open arrowheads] similar to those detected with antibodies against reelin and laminin [Fig. 2(D,H)].

We also assessed the expression of additional components of the cell cycle machinery and downstream effectors, including Cyclin E1, p15, p16, p18, p21, p27kip1, p57, Myc, and N-Myc, in both control and mutant brains, but were unable to detect obvious changes in the expression of any of these genes (Supporting Information Fig. 3 and data not shown).

The loss of Cyclin D2 expression in SVZ cells provides a plausible mechanism for the premature exit of SVZ cell from the cell cycle, since Cyclin D2 loss of function mice show reduced proliferation and an increase in cell cycle exit in the SVZ (Glickstein et al., 2009). However, we were puzzled by the acquisition of Cyclin D2 expression in the IZ, since these cells did not incorporate BrdU in Rac1 mutants and therefore did not appear to be progenitor cells. To assess the identity of the Cyclin D2-positive cells in the mutant IZ, we combined fluorescent digoxygenin (DIG) *in situ* hybridization using riboprobes against Cyclin D2 with immunohistochemistry using antibodies against Tbr2 to label SVZ cells and TuJ1 to label postmitotic neurons. The results of fluorescent DIG *in situ* hybridization recapitulated those using radioactive probes and revealed Cyclin D2 mRNA in the SVZ of controls [Fig. 5(E)], in the IZ of the Rac1-deficient brains [Fig. 5(F), arrow], and in the MZ of both mutants and controls [Fig. 5(E,F)]. Furthermore, higher power images [Fig. 5(G)] show that Cyclin D2-positive cells were positioned above the Tbr2-positive SVZ cells, indicating that the Cyclin D2 expressing cells were not intermediate SVZ progenitors. Instead, most cyclin D2-positive cells co-expressed TuJ1 [Fig. 5(H)], suggesting that these cells were postmitotic neurons that had inappropriately acquired Cyclin D2 expression. Comparisons of matching sections stained for BrdU [Fig. 5(I); 2-h BrdU pulse] or Cyclin D2 [Fig. 5(J); DIG *in situ*] revealed that the domain of BrdU-positive cells in the SVZ was localized below the cyclin D2 expression domain in the IZ. Collectively, these data suggest that the cyclin D2-expressing cells in the IZ are postmitotic neurons.

Rac1-Deficient Progenitors Can Still Give Rise to SVZ-Derived Upper Layer Neurons

Previous studies have revealed that many SVZ markers, such as Svet1, Cux1, and Cux2, are also expressed by upper layer neurons (Tarabykin et al., 2001; Nieto et al., 2004). Taken together with imaging experiments (Noctor et al., 2001; Noctor et al., 2002; Haubensak et al., 2004; Miyata et al., 2004), these data suggest that the SVZ is the primary neurogenic zone for neurons destined for layers 2–4. The severe reduction in proliferation and increased cell cycle exit within the SVZ in Rac1 mutants therefore suggests that the mutants might show altered expression of SVZ markers. To address this, we performed DIG *in situ* hybridization against the SVZ markers Svet1 [Fig. 6(A–F)], Cux1 (data not shown), and Cux2 [Fig. 6(G–L)] in controls and Rac-deficient brains at E17.5. We combined the fluorescent DIG probes with immunostaining for the SVZ marker Tbr2 (Englund et al., 2005). Svet1 mRNA was expressed in Rac1 mutants, although its expression domain appeared to extend more apically towards the VZ in mutants compared to controls [Fig. 6(A–E)]. This was similar to the expansion of Tbr2 expression into the VZ of mutants [Fig. 6(D,E); arrows]. Similarly, Cux2 mRNA expression was maintained in Rac1 mutants but extended further into the VZ [Fig. 6(J–L)] compared to controls [Fig. 6(G–I)]. Svet1, Cux1, and Cux2 mRNA expression was also maintained in the cortical plate of Rac1 mutants (Fig. 7); we detected an overall reduction in expression level of the three riboprobes tested, but this could be attributed to the reduced size of the mutant brains compared to controls. Together, these data suggest that the Rac1 mutants are able to form SVZ-derived upper layer neurons.

Foxg1-Cre;Rac1 mutant mice die around E18.5, which precludes a detailed analysis of the fates of late-generated neurons. To circumvent this problem, we crossed mice bearing the conditional allele of Rac1 with animals expressing a tamoxifen-inducible Cre under transcriptional control of the nestin promoter (Nestin-CreERT2; Imayoshi et al., 2006). In Nestin-CreERT2;Rac1 mice, activation of Cre by intraperitoneal administration of Tamoxifen during early corticogenesis leads to recombination in progenitors, as revealed by a Z/EG reporter (Novak et al., 2000) that marks recombined cells by EGFP expression [Fig. 8(A)]. The amount of Tamoxifen administered to pregnant dams can be used to titrate the percentage of recombined cells (Leone et al., 2003). We found that 2 mg Tamoxifen injected at E11.5 resulted in too many recombined neurons (data not shown), whereas 1 mg Tamoxifen injected at E11.5 resulted in an average of 100 recombined cells per visible field. This density of cells enabled us to assess the fates of Rac1-deficient cells at postnatal stages of cortical development.

EGFP-expressing cells were scattered over the entire cortical wall in both controls [Fig. 8(B)] and mutants [Fig. 8(C)]. We quantified the distribution of EGFP-expressing cells by dividing the cortical plate

into six equally spaced radial bins and plotting the percentage of EGFP-expressing cells in each bin for pyramidal neurons [Fig. 8(D), arrows in Fig. 8(E)] and non-pyramidal cells [which resemble interneurons and glia; Fig. 8(G), arrow in Fig. 8(F)] in mutant and control brains. Rac1 mutant pyramidal neurons showed a statistically significant bias towards deeper layers of the cortex compared to controls [bins 4 and

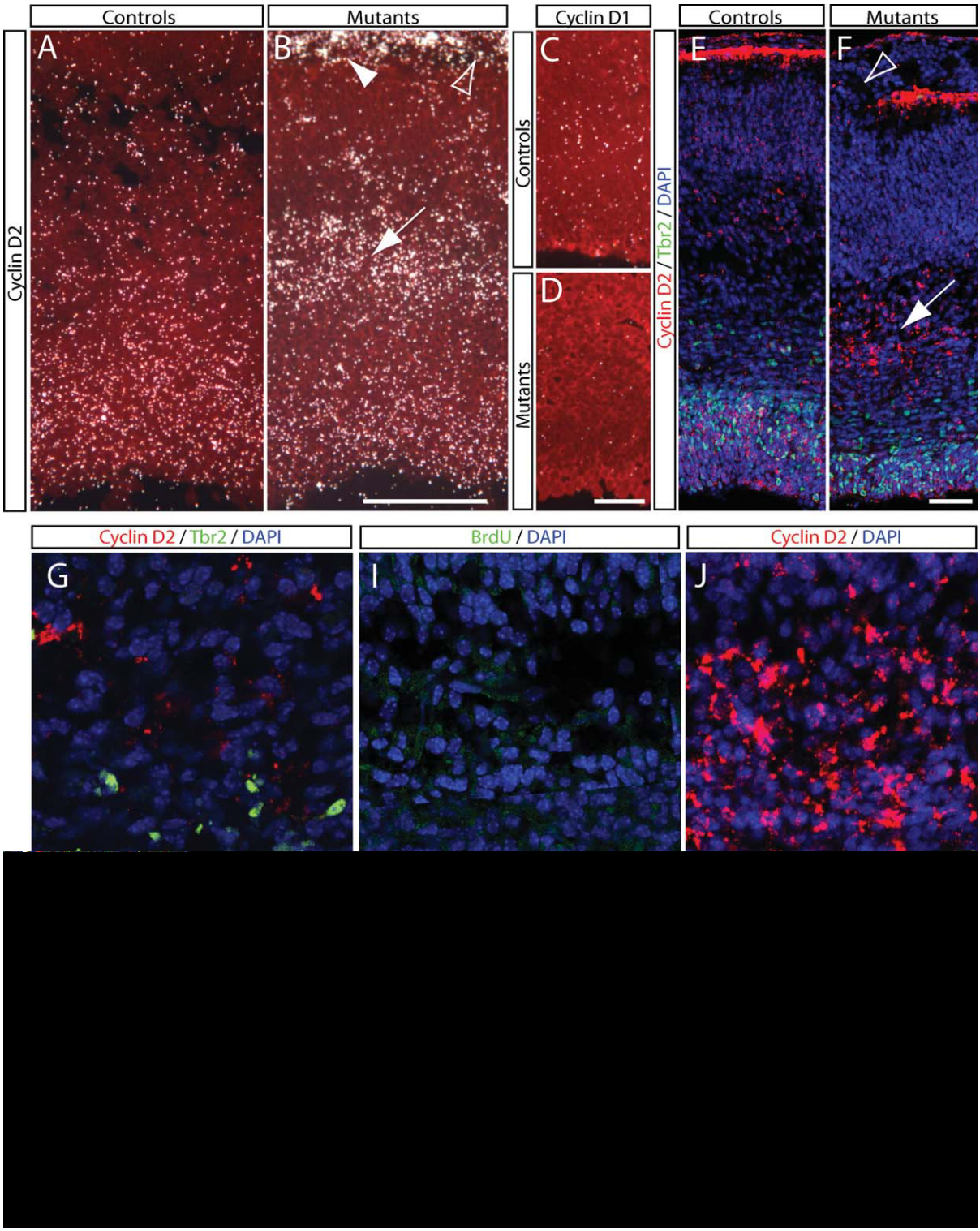

Figure 5

6, Fig. 8(D); $p < 0.005$ (bin 4), $p < 0.05$ (bin 6); $n =$ 4 controls and 3 mutants], and a non-significant trend away from more superficial layers [bin 2; Fig. 8(D); $p = 0.17$]. As expected, no significant difference was found for bin 1 between mutants and controls since the majority of the cells in this bin are early generated marginal zone cells which do not seem to be affected by the loss of Rac1. Nestin-CreERT2 should trigger recombination in cortical VZ progenitors that first generate pyramidal neurons then astrocytes (Walsh and Cepko, 1988; Williams et al., 1991; Reid et al., 1995; Noctor et al., 2008; reviewed in Kriegstein and Alvarez-Buylla, 2009), and in ganglionic eminence progenitors that produce EGFP-positive cortical interneurons (de Carlos et al., 1996; Anderson et al., 1997; Tamamaki et al., 1997; Lavdas et al., 1999; Sussel et al., 1999; Wichterle et al., 1999). We therefore assessed the distribution of non-pyramidal-shaped EGFP-positive cells (interneurons and glial cells) and found a significant increase in the percentage of recombined cells occupying the deepest bin [bin 6, Fig. 8(G); $p < 0.05$] compared to controls. Collectively, these data indicate that in the absence of Rac1, cortical progenitors are still able to generate upper layer neurons, but that there is a significant increase in the fraction of progeny found in the deep layers. Thus, Rac1 is not required for SVZ cells to acquire their appropriate identity or to generate upper layer neurons during development, but rather Rac1 plays an important role in regulating the fraction of SVZ cells that reenter versus quit the cell cycle during late stages of neurogenesis.

DISCUSSION

Progenitor cells in the cortical VZ and SVZ differ markedly in their morphologies, tissue organization, and mitotic behavior, and they produce neurons destined for different layers and phenotypes during development. Little is known about the signaling pathways that regulate these distinct patterns of proliferation and differentiation. Here, we show that the Rho GTPase Rac1 is required for the proliferation and regulation of cell cycle exit in SVZ progenitors and for survival of both SVZ and VZ progenitors. In the absence of Rac1, many fewer SVZ cells re-enter the cell cycle and instead show premature cell cycle exit and differentiation. Cyclin D2 expression, which is normally strong in the SVZ, is greatly reduced in Rac1 mutants. Surprisingly, upper layer neuron markers such as Svet1, Cux1, and Cux2 are still expressed, albeit at lower levels, in Rac1 mutants, suggesting that the loss of Rac1 by itself does not affect fate acquisition by upper layer neurons, but rather that Rac1 controls the proliferation of the SVZ progenitors that normally generate these neurons during development.

Defects in Proliferation and Cell Cycle Exit of SVZ Cells in Rac1-Deficient Forebrains

Progenitor cells in the SVZ are distinct from their VZ counterparts in that SVZ cells are loosely organized multipolar cells that undergo symmetric neurogenic

Figure 5 Changes in cyclin D1 and D2 expression in Rac1-deficient brains. A–D: Radioactive *in situ* hybridization against cyclin D1 and D2. A: Cyclin D2 is expressed in the VZ and SVZ at E17.5 in the developing forebrain of controls (expression signal in white; sections were counterstained with cresyl violet; red in A–D). B: In Rac1 mutants, cyclin D2 expression is reduced in the SVZ, and instead an ectopic band of expression is seen in the IZ (arrow). Cyclin D2 is also found in the marginal zone (arrowhead in B), and breaks therein are visible in the mutants (open arrowhead in B). C and D: Cyclin D1 is expressed weakly in the VZ at E17.5 in controls (C). In Rac1-mutants, cyclin D1 expression is markedly reduced (D). E and F: Fluorescent DIG *in situ* hybridization against cyclin D2 (red in E and F), combined with immunohistochemistry against the SVZ marker Tbr2 (green) confirms the radioactive *in situ* results shown in A and B. The ectopic band of Cyclin D2 expression in the mutant IZ is visible in the DIG *in situ* hybridization (arrow in F), as well as the breaks in the marginal zone (arrowhead in F) and neurons that have migrated past the pial endfeet. G: High-power magnification shows that mutant cells in the IZ that ectopically express cyclin D2 (red in G) do not coexpress Tbr2 (green in G). H: Double labeling of fluorescent DIG *in situ* hybridization against cyclin D2 (red) combined with immunohistochemistry against TuJ1 (green) shows that cyclin D2-positive cells are also positive for the neuronal marker TuJ1. I and J: High-power magnifications of a BrdU-stained mutant section (green in I; 2 h pulse), and a comparable section stained against the DIG cyclin D2 (red in J) show that none of the cyclin D2-positive cells in the IZ incorporate BrdU. Genotypes: controls are Foxg1-Cre^{+}; Rac1$^{fx/wt}$, mutants are Foxg1-Cre^{+}; Rac1$^{fx/fx}$. All sections are coronal sections of E17 embryos. Scale bars: 400 μm in B for A and B; 100 μm in D for C and D; 100 μm in F for E and F; 35 μm in H for G and H; 50 μm in J for I and J.

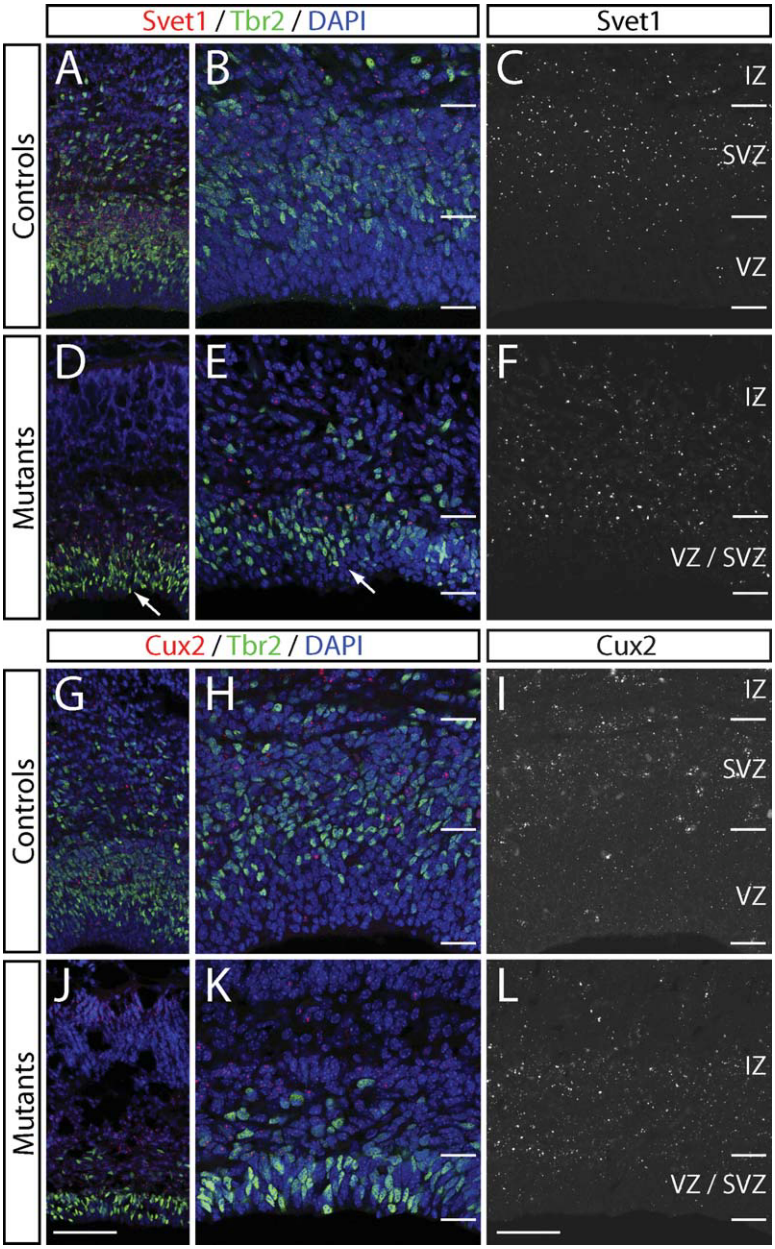

Figure 6 Rac1-deficient brains still express SVZ markers. Fluorescent DIG *in situ* hybridization against the SVZ marker Svet1 (A–F) combined with immunohistochemistry against the SVZ marker Tbr2 at E17.5. A–F: Svet1 expression (red in A, B, D, and E; white in C and F) and Tbr2 (green in A, B, D, and E) is shown in controls (A–C). Svet1 mRNA is still present in Rac1 mutants (D–F). Note the overall reduction in $Tbr2^{+}$ cells in the mutants and a shift in its expression pattern towards the apical surface (arrows in D and E) in the mutants. G–L: Cux2 *in situ* hybridization combined with Tbr2 immunohistochemistry. G–I: Cux2 (red in G, H, J, and K; white in I and L) and Tbr2 (green in G, H, J, and K) in controls (G–I) and Rac1 mutants (J–L) shows no obvious reduction in Cux2 expression in Rac1 mutants. Genotypes: controls are Foxg1-Cre^{+}; $Rac1^{fx/wt}$, mutants are Foxg1-Cre^{+}; $Rac1^{fx/fx}$. All sections are coronal sections of E17 embryos. Scale bars: 100 μm in J for A, D, G, and J; 50 μm in L for B, C, E, F, H, I, K, and L.

divisions. The VZ, in contrast, is tightly packed in a pseudostratified epithelium that shows a highly polarized radial organization; the cells undergo interkinetic nuclear migration during cell cycle progression and can divide symmetrically or asymmetrically. These differences suggest that the two cell populations

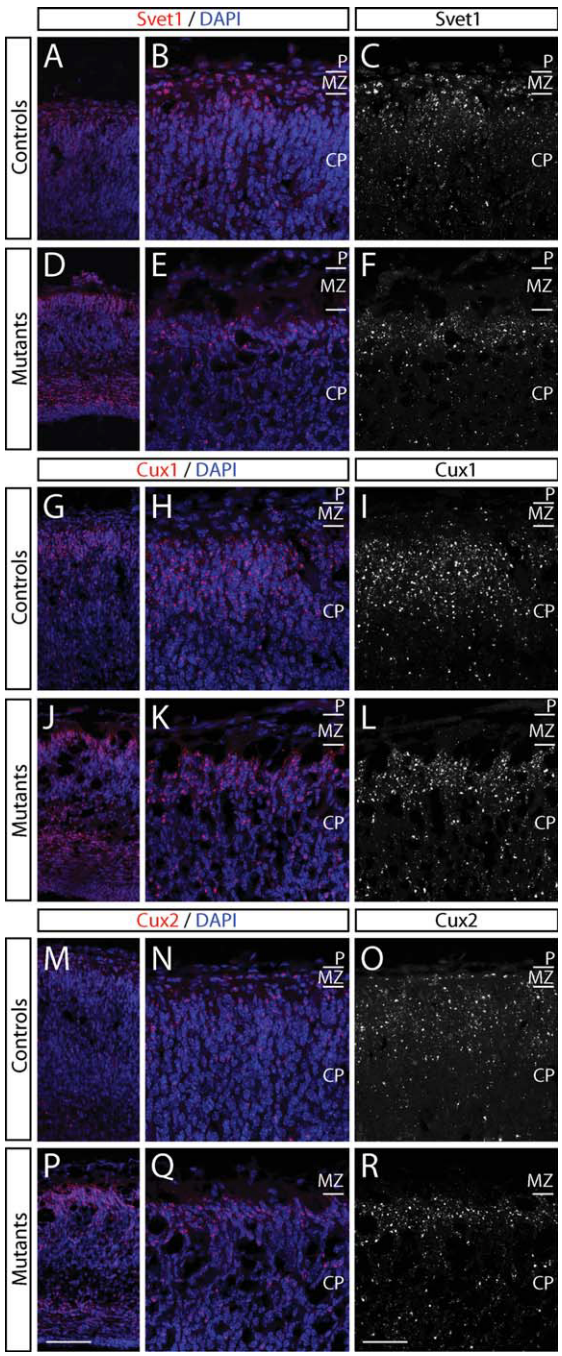

Figure 7 Rac1 mutants express upper layer neuron markers in the cortical plate at E17.5. Fluorescent DIG *in situ* hybridization against the upper layer markers Svet1, Cux-1, and Cux2 at E17.5. A–F: Svet1 expression (red in A, B, D, and E and white in C and F) in controls (A–C) and Rac1 mutants (D–F) shows that Rac1 mutants still form upper layer neurons. G–L: Cux-1 is expressed in the cortical plate of controls (G–I) and it is maintained in Rac1 mutants (J–L). Similarly, Cux2 expression in controls (M–O) and in mutants (P–R) is not obviously affected by loss of Rac1. Genotypes: all controls are Foxg1-Cre^{+}; Rac1$^{fx/wt}$, mutants are Foxg1-Cre^{+}; Rac1$^{fx/fx}$. Scale bars: 100 μm in P for A, D, G, J, M, and P; 50 μm in R for B, C, E, F, H, I, K, L, N, O, Q, and R.

employ distinct mechanisms for regulating proliferation and differentiation. Indeed, two recent publications have highlighted important regulators specific to SVZ but not VZ cells. When the homeodomain transcription factor Cux2 was knocked out in mice, progenitors in the SVZ overproliferated (Cubelos et al., 2008), whereas VZ cell were unaffected. Conversely, genetic deletion of the D-type cyclin D2, which is preferentially expressed by SVZ cells, reduced their proliferation and increased cell cycle exit (Glickstein et al., 2009).

Rac1 appears to regulate the organization, proliferation, and differentiation of SVZ cells, and the survival of both VZ and SVZ cells. At early stages of neurogenesis, the brains of control and mutant mice were similar in size and appearance, but by E14.5 the VZ and SVZ of Rac1 mutants had collapsed into a single fused zone, making a demarcation between them impossible. Loss of Rac1 leads to an increase in apoptosis over the entire cerebral wall at E14.5. We observed a high fraction of TUNEL-positive cells near the ventricular surface, presumably VZ or SVZ cells. These findings suggest that the reduced size of Rac1 mutant brains might be due to a significant amount of cell death occurring during early corticogenesis. By E17.5, the cerebral wall in Rac1 mutants was thinner than in wild-type controls, and the VZ/SVZ and IZ were all reduced in thickness. The failure of Rac1 mutants to establish the SVZ as a clear zone was further emphasized by the positions of Tbr2^{+} cells, which were found in more apical locations (towards the ventricle) in Rac1 mutants than in control brains.

At late stages of neurogenesis in Rac1 mutants, BrdU labeling experiments reveal that Tbr2^{+} progenitors failed to pause in the SVZ to proliferate, as they do in control mice, and instead continued to migrate into the IZ. Quit fraction analyses revealed that Tbr2^{+} cells were significantly more likely to exit the cell cycle in Rac1 mutants, leading to precocious differentiation of neurons derived from the SVZ progenitor pool. In contrast, Tbr2^{-} VZ cells showed no difference in BrdU incorporation or cell cycle exit, leading us to conclude that the proliferative behavior of these cells is unaffected by the loss of Rac1. The decreased proliferation and premature differentiation of SVZ cells is likely to be responsible, in part or in whole, for the decreased size of Rac1 mutant brains compared to controls. Although previous work has shown that Rac1 regulates axon guidance in the developing forebrain, Rac1 is not required for axon outgrowth (Chen et al., 2007), suggesting the reduction in brain size may be primarily the consequence of decreased neurogenesis.

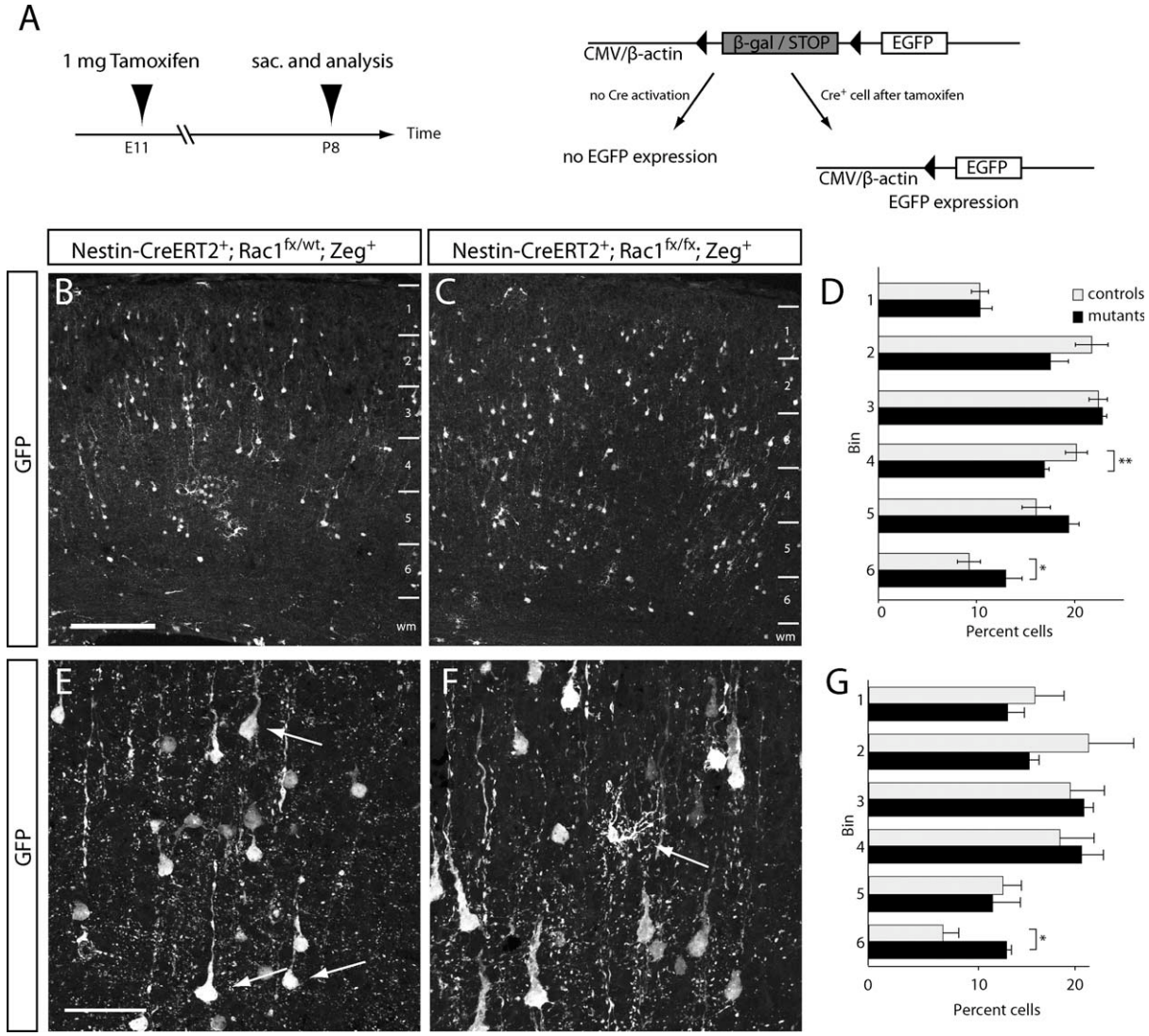

Figure 8 Mosaic Rac1-deficient brains can still give rise to pyramidal neurons of all layers. A: Schematic representation of the experimental approach. Rac1 was deleted in a low percentage of progenitor cells at E11.5 using a single 1 mg i.p. injection of Tamoxifen into pregnant dams. Nestin-CreERT2-mediated recombination leads to excision of the transcriptional stop cassette in the Z/EG reporter leading to EGFP expression in recombined progenitors which subsequently gave rise to neurons. Pups of injected pregnant mothers were analyzed at P8. B and C: Representative images of sections from a Tamoxifen-treated control (B; Nestin-CreERT2^{+}; Rac1$^{fx/wt}$; Zeg^{+}) and mutant (C; Nestin-CreERT2^{+}; Rac1$^{fx/fx}$; Zeg^{+}). Z/EG-based EGFP-expressing cells (white in B and C) can be seen over the entire cortical wall. No obvious difference in the distribution of EGFP expressing neurons was found between mutants and controls. D: Quantification of the distribution of EGFP-expressing pyramidal neurons in controls (white bars) and mutants (black bars). A statistically significant increase was found in the percentage of mutant cells in the deepest bin 6 (*$p < 0.05$), and concomitantly a reduction of mutant cells in bin 4 (**$p < 0.005$) and a non-significant trend towards a reduction in upper layer bin 2 ($p = 0.17$) compared to controls. E and F: High-power magnification representative images of EGFP-expressing pyramidal neurons (E: arrows) and non-pyramidal cells (F: arrow) that were used to identify cell types for quantification. G: Quantification of layer distribution of EGFP-expressing non-pyramidal cells (interneurons and glial cells) shows an increase of EGFP-positive cells in the deepest bin 6 compared to controls (*$p < 0.05$). *$p < 0.05$, **$p < 0.005$, student's t test. $n = 4$ control and 3 mutant animals. Error bars show Mean ± SE. Scale bars: 200 μm in B for B and C; 50 μm in E for E and F.

Rac1 appears to regulate proliferation and cell cycle exit by affecting the expression of core components of the cell cycle machinery. During the G1 phase of the cell cycle, D-type cyclins enable cells to progress through a key cell cycle checkpoint; successful passage allows E-type cyclins to accumulate before the initiation of S phase (Koff et al., 1991; Lew et al., 1991; Sherr, 1993). Interestingly, the near-complete loss of cyclin D2 mRNA expression in the SVZ of Rac1 mutants and concomitant changes in SVZ cell behavior phenocopy those observed in cyclin D2 knockout mice. The loss of cyclin D2 during forebrain development leads to a decrease in the number of $Tbr2^+$ SVZ progenitors, a reduction in their proliferation, and increased cell cycle exit (Glickstein et al., 2009). During normal development, cyclin D2 expression is acquired as cells start to lose Pax6 expression and turn on Tbr2, a transition that correlates with the specification of the SVZ (Glickstein et al., 2009). In cyclin D2 knockout mice, SVZ progenitors increased their expression of the Cdk inhibitor p27 and showed a reduction in phosphorylation of the retinoblastoma protein Rb (Glickstein et al., 2009), both of which should disrupt progression through the G1-S transition in the cell cycle. p27 mRNA expression was not obviously altered in Rac1 mutants, but regulation of p27 can occur both at the levels of translation/protein stability and transcription (reviewed in Alkarain and Slingerland, 2004). It is conceivable that p27 may have been altered post-transcriptionally in Rac1 mutant progenitors.

It is not clear whether the normal acquisition of cyclin D2 expression in SVZ cells triggers a specific change in their mitotic behavior (which is distinct from that in polarized VZ progenitors that express cyclin D1), or whether cyclin D2 is required for cell cycle progression in the SVZ because other D-type cyclins cannot compensate for its absence. However, the similar changes in proliferation and cell cycle exit in Rac1 and cyclin D2 mutants suggests that Rac1 acts genetically upstream of cyclin D2 in the SVZ lineage. Cyclin D2 and Rac1 have previously been linked in B lymphocytes, since B cells that lack the Rac1-specific guanine nucleotide exchange factor Vav fail to proliferate due to a failure to induce cyclin D2 (Glassford et al., 2001). This raises the intriguing possibility that a Vav family member may regulate Rac1 activity in the developing SVZ.

Although the loss of cyclin D2 expression in SVZ cells appears to account for much of the Rac1 mutant phenotype, we were surprised to observe cyclin D2 expression in postmitotic $Tbr2^-$ cells in the IZ. Rac1 is thus not absolutely required for cells to express cyclin D2, and must instead regulate the timing of its expression. We did not observe excess numbers of ectopically proliferating cells in the IZ, which suggests that the late onset of cyclin D2 expression failed to trigger cell cycle reentry. Indeed, it is likely that these cells have progressed far enough along the neuronal differentiation program that the upregulation of cyclin D2 is insufficient to push the cells into reentering the cell cycle.

Rac1-Deficient Progenitors Produce Upper Layer Neurons

Rac1 mutants continue to express upper layer neuronal markers, including Svet1, Cux1, and Cux2, which are also expressed by SVZ cells. This observation suggests that cell fate decisions are not affected by the loss of Rac1, but instead the shrinkage of the SVZ reflects a reduction in the numbers of these progenitors. If SVZ cells are the sole or primary source of upper layer neurons, one would predict that Rac1 mutant mice should show a quantitative deficit in the production of late-generated neurons and relatively normal deep layer neurogenesis. *In situ* hybridization for upper layer markers revealed decreased expression within the cortical plate of Rac1 mutants, but neonatal lethality precluded a detailed quantification of upper layer production in these animals. To circumvent this problem, we used a tamoxifen-inducible Cre under transcriptional control of the nestin promoter. A single administration of 1 mg Tamoxifen resulted in recombination in a relatively low number of neurons, whereas doses higher than 1 mg interfered with perinatal survival of the pups. These experiments revealed that Rac1-deficient cells can generate upper layer neurons, and quantification of the positions of recombined neurons suggested a trend towards deep layer production at the expense of the upper layers. It is not clear whether tamoxifen produced an incomplete recombination of the Rac1 locus, which would underestimate the effects of the mutation on upper layer neurogenesis, whether the smaller number of SVZ progenitors somehow compensated for the loss of Rac1 and generated near-normal numbers of upper layer cells, or whether upper layer neurons in these mice were actually derived from VZ progenitors.

Migration Defects in Rac1 Mutants are Secondary to Defects in the Basal Lamina

The morphological defects found in the Rac1 mutants include migration defects that are reminiscent of

many cobblestone lissencephalies (reviewed in Olson and Walsh, 2002). The defects include a laminar disorganization, which is manifested by the expression of the deep layer marker Ctip2 in neurons just beneath the pial surface. The mutant brains display breaks in the basal lamina that are associated with disorganized radial glial fibers, which extend past the marginal zone into the pericerebral space. It is tempting to speculate that Rac1 plays a role in this interaction between the deposition of the basement membrane and the stabilization of the pial endfeet of radial glial cells. Intriguingly, a recent article suggested a signaling pathway in MDCK cells in which activation of beta1-integrins requires Rac1 activation and laminin organization at the basement membrane (Yu et al., 2005). The severe reduction in olfactory bulbs in the Rac1 mutants suggests that either the migration of neurons from the rostral migratory stream or proliferation during bulb evagination could be affected by the loss of Rac1, but we have not further investigated these findings.

Distinct Roles for Rho Family GTPases in Cortical Development

A forebrain-specific loss of Cdc42, another member of the Rho GTPase family, leads to loss of adherens junctions and apical polarity complex (Cappello et al., 2006). In contrast, the loss of Rac1 does not affect either adherens junctions or the apical polarity complex, suggesting that junction formation and cell polarity specifically require Cdc42 but not Rac1 during development. Similarly, the expression of phosphorylated PAK at the apical surface of VZ progenitors is affected by the loss of Cdc42 but not Rac1, confirming the requirement for Cdc42 function in radial glia cells. Previous work has shown that loss of Cdc42 leads to a disorganization of the radial glia (Cappello et al., 2006 and our own unpublished data), with Cdc42-deficient cells retracting their radial processes and delaminating away from the apical surface. Consequently, Cdc42-mutant forebrains show an increase in basal mitoses, which interestingly are associated with the increased expression of the SVZ markers Svet1, Btg2, and Cux2 (Cappello et al., 2006). It is unclear whether the upregulation of SVZ markers under these circumstances is a secondary effect of radial glia cells proceeding along their default differentiation process and thereby giving rise to SVZ progenitors, or whether they undergo an active fate change that leads to the upregulation of the markers.

When considered along with previous studies, our data suggest that the Rho family GTPases Rac1 and Cdc42 subserve distinct and—at least in part—nonoverlapping roles in cortical progenitor cells. Cdc42 is required for the maintenance of polarity and normal proliferation in radial glial cells of the VZ (Cappello et al., 2006), whereas Rac1 regulates survival of both VZ and SVZ progenitors, proliferation, and cell cycle exit by SVZ progenitors by controlling the expression of cyclin D2. In light of these observations, it is tempting to speculate that Rac1 has been used during evolution to promote the radial expansion of the mammalian cortex by regulating the proliferative behavior of SVZ progenitors.

The authors thank C. Kaznowski for technical help with critical experiments.

REFERENCES

Alberti S, Krause SM, Kretz O, Philippar U, Lemberger T, Casanova E, Wiebel FF, et al. 2005. Neuronal migration in the murine rostral migratory stream requires serum response factor. Proc Natl Acad Sci USA 102:6148–6153.

Alcamo EA, Chirivella L, Dautzenberg M, Dobreva G, Fariñas I, Grosschedl R, McConnell SK. 2008. Satb2 regulates callosal projection neuron identity in the developing cerebral cortex. Neuron 57:364–377.

Alkarain A, Slingerland J. 2004. Deregulation of p27 by oncogenic signaling and its prognostic significance in breast cancer. Breast Cancer Res 6:13–21.

Anderson SA, Eisenstat DD, Shi L, Rubenstein JL. 1997. Interneuron migration from basal forebrain to neocortex: Dependence on Dlx genes. Science 278:474–476.

Arlotta P, Molyneaux BJ, Chen J, Inoue J, Kominami R, Macklis JD. 2005. Neuronal subtype-specific genes that control corticospinal motor neuron development *in vivo*. Neuron 45:207–221.

Bayer SA, Altman J, Dai XF, Humphreys L. 1991. Planar differences in nuclear area and orientation in the subventricular and intermediate zones of the rat embryonic neocortex. J Comp Neurol 307:487–498.

Beggs HE, Schahin-Reed D, Zang K, Goebbels S, Nave KA, Gorski J, Jones KR, et al. 2003. FAK deficiency in cells contributing to the basal lamina results in cortical abnormalities resembling congenital muscular dystrophies. Neuron 40:501–514.

Benitah SA, Frye M, Glogauer M, Watt FM. 2005. Stem cell depletion through epidermal deletion of Rac1. Science 309:933–935.

Britanova O, Akopov S, Lukyanov S, Gruss P, Tarabykin V. 2005. Novel transcription factor Satb2 interacts with matrix attachment region DNA elements in a tissue-specific manner and demonstrates cell-type-dependent expression in the developing mouse CNS. Eur J Neurosci 21:658–668.

Britanova O, de Juan Romero C, Cheung A, Kwan KY, Schwark M, Gyorgy A, Vogel T, et al. 2008. Satb2 is a postmitotic determinant for upper-layer neuron specification in the neocortex. Neuron 57:378–392.

Cappello S, Attardo A, Wu X, Iwasato T, Itohara S, Wilsch-Bräuninger M, Eilken HM, et al. 2006. The Rho-GTPase cdc42 regulates neural progenitor fate at the apical surface. Nat Neurosci 9:1099–1107.

Chen B, Schaevitz LR, McConnell SK. 2005. Fezl regulates the differentiation and axon targeting of layer 5 subcortical projection neurons in cerebral cortex. Proc Natl Acad Sci USA 102:17184–17189.

Chen L, Liao G, Waclaw RR, Burns KA, Linquist D, Campbell K, Zheng Y, et al. 2007. Rac1 controls the formation of midline commissures and the competency of tangential migration in ventral telencephalic neurons. J Neurosci 27:3884–3893.

Chen L, Melendez J, Campbell K, Kuan CY, Zheng Y. 2009. Rac1 deficiency in the forebrain results in neural progenitor reduction and microcephaly. Dev Biol 325: 162–170.

Chenn A, McConnell SK. 1995. Cleavage orientation and the asymmetric inheritance of Notch1 immunoreactivity in mammalian neurogenesis. Cell 82:631–641.

Chenn A, Walsh CA. 2003. Increased neuronal production, enlarged forebrains and cytoarchitectural distortions in beta-catenin overexpressing transgenic mice. Cereb Cortex 13:599–606.

Chenn A, Zhang YA, Chang BT, McConnell SK. 1998. Intrinsic polarity of mammalian neuroepithelial cells. Mol Cell Neurosci 11:183–193.

Chrostek A, Wu X, Quondamatteo F, Hu R, Sanecka A, Niemann C, Langbein L, et al. 2006. Rac1 is crucial for hair follicle integrity but is not essential for maintenance of the epidermis. Mol Cell Biol 26:6957–6970.

Cubelos B, Sebastián-Serrano A, Kim S, Moreno-Ortiz C, Redondo JM, Walsh CA, Nieto M. 2008. Cux-2 controls the proliferation of neuronal intermediate precursors of the cortical subventricular zone. Cereb Cortex 18:1758–1770.

de Carlos JA, López-Mascaraque L, Valverde F. 1996. Dynamics of cell migration from the lateral ganglionic eminence in the rat. J Neurosci 16:6146–6156.

Englund C, Fink A, Lau C, Pham D, Daza RA, Bulfone A, Kowalczyk T, et al. 2005. Pax6, Tbr2, and Tbr1 are expressed sequentially by radial glia, intermediate progenitor cells, and postmitotic neurons in developing neocortex. J Neurosci 25:247–251.

Etienne-Manneville S, Hall A. 2002. Rho GTPases in cell biology. Nature 420:629–635.

Frantz GD, Bohner AP, Akers RM, McConnell SK. 1994. Regulation of the POU domain gene SCIP during cerebral cortical development. J Neurosci 14:472–485.

Glassford J, Holman M, Banerji L, Clayton E, Klaus GG, Turner M, Lam EW. 2001. Vav is required for cyclin D2 induction and proliferation of mouse B lymphocytes activated via the antigen Receptor. J Biol Chem 276:41040–41048.

Glickstein SB, Alexander S, Ross ME. 2007. Differences in cyclin D2 and D1 protein expression distinguish forebrain progenitor subsets. Cereb Cortex 17:632–642.

Glickstein SB, Monaghan JA, Koeller HB, Jones TK, Ross ME. 2009. Cyclin D2 is critical for intermediate progenitor cell proliferation in the embryonic cortex. J Neurosci 29:9614–9624.

Graus-Porta D, Blaess S, Senften M, Littlewood-Evans A, Damsky C, Huang Z, Orban P, et al. 2001. Beta1-class integrins regulate the development of laminae and folia in the cerebral and cerebellar cortex. Neuron 31:367–379.

Halfter W, Dong S, Yip YP, Willem M, Mayer U. 2002. A critical function of the pial basement membrane in cortical histogenesis. J Neurosci 22:6029–6040.

Haubensak W, Attardo A, Denk W, Huttner WB. 2004. Neurons arise in the basal neuroepithelium of the early mammalian telencephalon: A major site of neurogenesis. Proc Natl Acad Sci USA 101:3196–3201.

Hébert JM, Lin M, Partanen J, Rossant J, McConnell SK. 2003. FGF signaling through FGFR1 is required for olfactory bulb morphogenesis. Development 130:1101–1111.

Hébert JM, McConnell SK. 2000. Targeting of cre to the Foxg1 (BF-1) locus mediates loxP recombination in the telencephalon and other developing head structures. Dev Biol 222:296–306.

Imayoshi I, Ohtsuka T, Metzger D, Chambon P, Kageyama R. 2006. Temporal regulation of Cre recombinase activity in neural stem cells. Genesis 44:233–238.

Knoepfler PS, Cheng PF, Eisenman RN. 2002. N-myc is essential during neurogenesis for the rapid expansion of progenitor cell populations and the inhibition of neuronal differentiation. Genes Dev 16:2699–2712.

Koff A, Cross F, Fisher A, Schumacher J, Leguellec K, Philippe M, Roberts JM. 1991. Human cyclin E, a new cyclin that interacts with two members of the CDC2 gene family. Cell 66:1217–1228.

Kriegstein A, Alvarez-Buylla A. 2009. The glial nature of embryonic and adult neural stem cells. Annu Rev Neurosci 32:149–184.

Lavdas AA, Grigoriou M, Pachnis V, Parnavelas JG. 1999. The medial ganglionic eminence gives rise to a population of early neurons in the developing cerebral cortex. J Neurosci 19:7881–7888.

Leone DP, Genoud S, Atanasoski S, Grausenburger R, Berger P, Metzger D, Macklin WB, et al. 2003. Tamoxifen-inducible glia-specific Cre mice for somatic mutagenesis in oligodendrocytes and Schwann cells. Mol Cell Neurosci 22:430–440.

Leone DP, Srinivasan K, Chen B, Alcamo E, McConnell SK. 2008. The determination of projection neuron identity in the developing cerebral cortex. Curr Opin Neurobiol 18:28–35.

Lew DJ, Dulic V, Reed SI. 1991. Isolation of three novel human cyclins by rescue of G1 cyclin (Cln) function in yeast. Cell 66:1197–1206.

Manser E, Leung T, Salihuddin H, Zhao ZS, Lim L. 1994. A brain serine/threonine protein kinase activated by Cdc42 and Rac1. Nature 367:40–46.

Miyata T, Kawaguchi A, Okano H, Ogawa M. 2001. Asymmetric inheritance of radial glial fibers by cortical neurons. Neuron 31:727–741.

Miyata T, Kawaguchi A, Saito K, Kawano M, Muto T, Ogawa M. 2004. Asymmetric production of surface-dividing and non-surface-dividing cortical progenitor cells. Development 131:3133–3145.

Nieto M, Monuki ES, Tang H, Imitola J, Haubst N, Khoury SJ, Cunningham J, et al. 2004. Expression of Cux-1 and Cux-2 in the subventricular zone and upper layers II-IV of the cerebral cortex. J Comp Neurol 479:168–180.

Noctor SC, Flint AC, Weissman TA, Dammerman RS, Kriegstein AR. 2001. Neurons derived from radial glial cells establish radial units in neocortex. Nature 409:714–720.

Noctor SC, Flint AC, Weissman TA, Wong WS, Clinton BK, Kriegstein AR. 2002. Dividing precursor cells of the embryonic cortical ventricular zone have morphological and molecular characteristics of radial glia. J Neurosci 22:3161–3173.

Noctor SC, Martínez-Cerdeño V, Ivic L, Kriegstein AR. 2004. Cortical neurons arise in symmetric and asymmetric division zones and migrate through specific phases. Nat Neurosci 7:136–144.

Noctor SC, Martínez-Cerdeño V, Kriegstein AR. 2008. Distinct behaviors of neural stem and progenitor cells underlie cortical neurogenesis. J Comp Neurol 508:28–44.

Novak A, Guo C, Yang W, Nagy A, Lobe CG. 2000. Z/EG, a double reporter mouse line that expresses enhanced green fluorescent protein upon Cre-mediated excision. Genesis 28:147–155.

Olenik C, Aktories K, Meyer DK. 1999. Differential expression of the small GTP-binding proteins RhoA, RhoB, Cdc42u and Cdc42b in developing rat neocortex. Brain Res Mol Brain Res 70:9–17.

Olson EC, Walsh CA. 2002. Smooth, rough and upside-down neocortical development. Curr Opin Genet Dev 12:320–327.

Rakic P. 2003a. Developmental and evolutionary adaptations of cortical radial glia. Cereb Cortex 13:541–549.

Rakic P. 2003b. Elusive radial glial cells: Historical and evolutionary perspective. Glia 43:19–32.

Reid CB, Liang I, Walsh C. 1995. Systematic widespread clonal organization in cerebral cortex. Neuron 15:299–310.

Ross ME, Carter ML, Lee JH. 1996. MN20, a D2 cyclin, is transiently expressed in selected neural populations during embryogenesis. J Neurosci 16:210–219.

Sherr CJ. 1993. Mammalian G1 cyclins. Cell 73:1059–1065.

Srinivasan K, Roosa J, Olsen O, Lee SH, Bredt DS, McConnell SK. 2008. MALS-3 regulates polarity and early neurogenesis in the developing cerebral cortex. Development 135:1781–1790.

Sugihara K, Nakatsuji N, Nakamura K, Nakao K, Hashimoto R, Otani H, Sakagami H, et al. 1998. Rac1 is required for the formation of three germ layers during gastrulation. Oncogene 17:3427–3433.

Sussel L, Marin O, Kimura S, Rubenstein JL. 1999. Loss of Nkx2.1 homeobox gene function results in a ventral to dorsal molecular respecification within the basal telencephalon: Evidence for a transformation of the pallidum into the striatum. Development 126:3359–3370.

Tamamaki N, Fujimori KE, Takauji R. 1997. Origin and route of tangentially migrating neurons in the developing neocortical intermediate zone. J Neurosci 17: 8313–8323.

Tarabykin V, Stoykova A, Usman N, Gruss P. 2001. Cortical upper layer neurons derive from the subventricular zone as indicated by Svet1 gene expression. Development 128:1983–1993.

Voss AK, Britto JM, Dixon MP, Sheikh BN, Collin C, Tan SS, Thomas T. 2008. C3G regulates cortical neuron migration, preplate splitting and radial glial cell attachment. Development 135:2139–2149.

Walsh C, Cepko CL. 1988. Clonally related cortical cells show several migration patterns. Science 241:1342–1345.

Wianny F, Real FX, Mummery CL, Van Rooijen M, Lahti J, Samarut J, Savatier P. 1998. G1-phase regulators, cyclin D1, cyclin D2, and cyclin D3: Up-regulation at gastrulation and dynamic expression during neurulation. Dev Dyn 212:49–62.

Wichterle H, Garcia-Verdugo JM, Herrera DG, Alvarez-Buylla A. 1999. Young neurons from medial ganglionic eminence disperse in adult and embryonic brain. Nat Neurosci 2:461–466.

Williams BP, Read J, Price J. 1991. The generation of neurons and oligodendrocytes from a common precursor cell. Neuron 7:685–693.

Yu W, Datta A, Leroy P, O'Brien LE, Mak G, Jou TS, Matlin KS, et al. 2005. Beta1-integrin orients epithelial polarity via Rac1 and laminin. Mol Biol Cell 16:433–445.

Zardoya R, Meyer A. 2001. The evolutionary position of turtles revised. Naturwissenschaften 88:193–200.

Zhang B, Zhang Y, Shacter E. 2003. Caspase 3-mediated inactivation of rac GTPases promotes drug-induced apoptosis in human lymphoma cells. Mol Cell Biol 23:5716–5725.

Zhang B, Zhang Y, Shacter E. 2004. Rac1 inhibits apoptosis in human lymphoma cells by stimulating Bad phosphorylation on Ser-75. Mol Cell Biol 24:6205–6214.